ORIGINAL ARTICLE

CrossMark

Monitoring the Instant Creation of a New Fluorescent Signal for Evaluation of DNA Conformation Based on Intercalation Complex

Ahmet T. Uzumcu[1] · Orhan Guney[1] · Oguz Okay[1]

© Springer Science+Business Media, LLC, part of Springer Nature 2018

Abstract

Here we report the monitoring the instant creation of a new fluorescent signal (FS) aroused from a positively charged water-soluble fluorogenic probe, ethidium bromide (EtBr) in the presence of a radical initiator, ammonium persulfate (APS) and an accelerator, tetraethylmetilendiamine (TEMED) for evaluation of deoxyribonucleic acid (DNA) conformation. The results revealed that the occurred FS ($\lambda_{ex} = 430$ nm; $\lambda_{max} = 525$ nm) is a reduced form of EtBr ($\lambda_{ex} = 480$ nm; $\lambda_{max} = 617$ nm) and it is completely distinct from hydroethidine ($\lambda_{ex} = 350$ nm; $\lambda_{max} = 430$ nm), which is two-electron reduced form of EtBr. It was noticed that EtBr was reduced to a new FS during the polymerization of N, N dimethyacrylamide (DMAA) too, at 25 °C in the presence of APS and TEMED or at 55 °C with only APS, and the rate of formation of FS was increased upon treatment time. The effect of nanoclays such as Laponite XLG® and Laponite XLS®, which provide a protective environment for DNA in nature, were also investigated through the reduction process of EtBr in the absence and presence of a water soluble monomer DMAA. We demonstrated that DNA conformation might be evaluated by monitoring FS effectuated during the reduction of EtBr in the presence of nanoclays having positively and negatively charged surfaces. Protective property of DNA against the formation of reduced product was elucidated by carrying out the polymerization at 55 °C. The results revealed that the monitoring of formation of FS in the presence of radical initiator could lead to elucidate the conformation of DNA upon formation of intercalator complex.

Keywords EtBr · DNA conformation · Intercalation complex · Nanoclay

Introduction

Fluorescent probes, which are of great importance for the improvement of biological imaging systems and assays, are requisite tools for biological chemistry and being used almost everywhere as tags for biomolecules, enzyme substrates, environmental markers, and cellular stains [1–3]. Ethidium bromide (EtBr) is widely utilized as a fluorescent probe for the determination of DNA conformation or interaction of DNA with physiologically important molecules [4–7]. Fluorescence intensity of free EtBr is weak but enhanced when it intercalates between the adjacent base pairs within the strands of DNA thanks to the prevention of the consisted hydrophobic micro-environment from the fluorescent quenchers such as oxygen or water, upon complexation [8–11]. By intercalation, fluorescence quantum yield of EtBr drastically increases and forms a complex with DNA by displaying an optical activity in the visible region [12, 13].

Increasing interest has recently been dedicated to synthetic organic molecules, especially anti-viral and anti-cancer drugs which are able to interact with DNA, arising from electrostatic interaction, intercalation between base pairs of DNA, or adhering to the groove of DNA [14–17]. Dihydroethidium also known as hydroethidine (HE) is the two-electron reduced form of EtBr and is converted (dehydrogenated) into EtBr inside the living cell, which then intercalates with DNA [18–20] and its fluorescence emission at 617 nm greatly enhances when excited at 530 nm. To investigate the oxidative stress, reactive oxygen species in cellular systems are determined by using HE as a fluorescent probe since oxidation product of HE strongly fluoresces upon interaction with DNA, making them easily detectable in cells [18, 19, 21]. The reduction of EtBr to HE was directly demonstrated by disappearance of the absorbance of

✉ Orhan Guney
  oguney@itu.edu.tr

✉ Oguz Okay
  okayo@itu.edu.tr

[1] Departments of Chemistry and Polymer Science & Technology, Istanbul Technical University, Maslak, 34469 Istanbul, Turkey

Scheme 1 Synthesis of HE by using EtBr
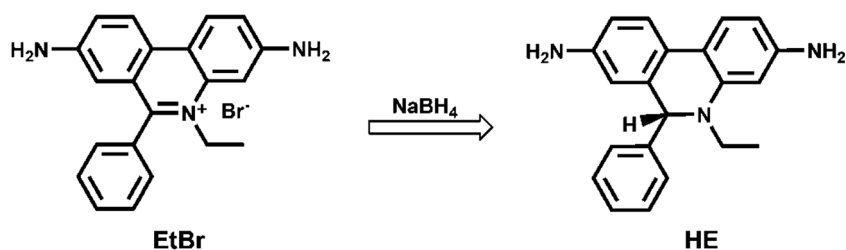
In this study, UV-vis and fluorescence spectroscopy techniques were used to gain insight into the reduction product of EtBr during the free radical polymerization of DMAA and to enlighten the conformational changes of DNA upon interaction with an intercalator molecule in the absence and presence of nanoclay.
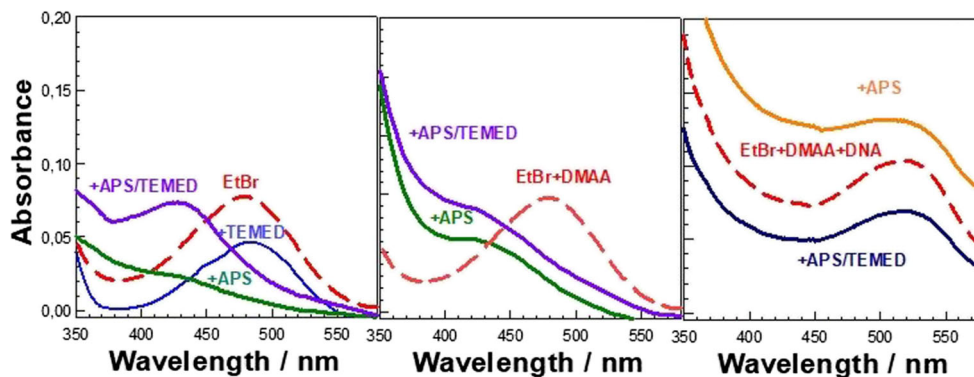
Materials and Methods

Materials

Ethidium bromide (EtBr), Deoxyribonucleic acid sodium salt (DNA) of salmon testes (~2000 base pairs), N,N,N,N′-tetramethylethylenediamine (TEMED), Dimethyl sulfoxide (DMSO) and N-N Dimethylacrylamide (DMAA) were purchased from Sigma and used as received. Ammonium persulfate (APS) was obtained from Fluka. Sodium borohydride (NaBH$_4$) was purchased from Sigma-Aldrich. The synthetic hectorite clays, Laponite XLG (Mg$_{5.34}$Li$_{0.66}$- Si$_8$O$_{20}$(OH)$_4$Na$_{0.66}$) and Laponite XLS (92.32 wt% of Mg$_{5.34}$Li$_{0.66}$- Si$_8$O$_{20}$(OH)$_4$Na$_{0.66}$ and 7.68 wt% of Na$_4$P$_2$O$_7$) were kindly provided by Rockwood Ltd.

Concentration and Functions of Materials

The concentrations of fluorogenic probe, EtBr (10 μM), the monomer, DMAA (1.0 M), the initiator, APS (3.51 mM) and the accelerator, TEMED (0.08 $v/v\%$) were fixed for all of the prepared samples. The concentration of ds-DNA was set to 2 $w/v\%$ while Laponite content was fixed to 3 w/v% throughout all measurements.

Synthesis of Hydroethidium

Hydroethidium (HE) was prepared as follows: 54 mg of NaBH$_4$ was added into 100 mg of EtBr, which was previously dissolved in 2 ml absolute methanol at 0 °C under nitrogen atmosphere in dark condition. After 20 h stirring, methanol was evaporated under vacuum and 3 ml of 3 $v/v\%$ NaOH solution was added. The precipitate was extracted several times with ether and washed with water. The precipitate was dried over anhydrous sodium sulfate and then recrystallized in ether to yield a light brown powder (Scheme 1).
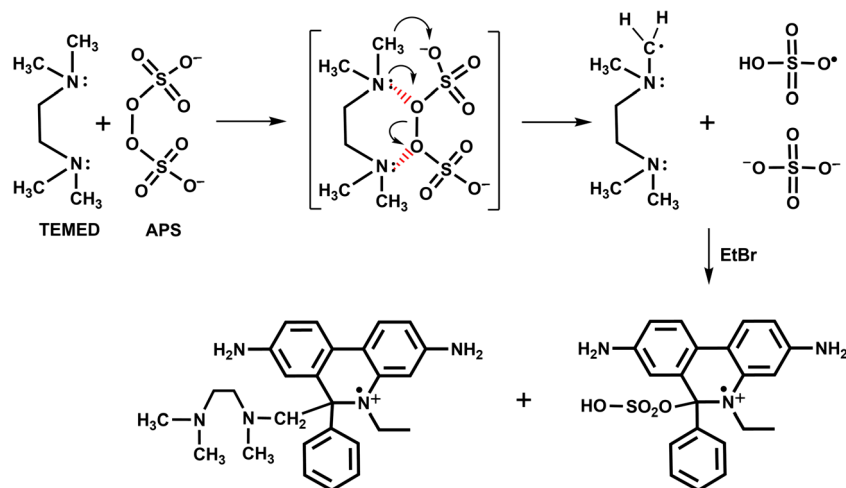
Fluorescence and UV-Vis Measurements

The fluorescence spectra of ethidium bromide (EtBr) were recorded on a Carry eclipse spectrofluorometer equipped with a thermostated cell holder. The excitation and emission slit widths were adjusted to 5 nm. The measurements were performed at various excitation wavelengths; 430, 475 and 530 nm and fluorescence spectra were recorded as a function of time. The UV-Vis spectra were obtained from a VWR UV-1600 PC spectrophotometer and the data were recorded via PC software.

Results and Discussion

Absorption Spectra of EtBr upon Addition of Diverse Reagents

Fig. 1a shows UV absorption spectra of 10 μM aqueous EtBr solution without and with the additives APS,

Fig. 1 UV absorption spectra of 10 μM aqueous EtBr solution with various additives. (**a**): EtBr alone (dashed curve) and after addition of APS, TEMED and APS/TEMED (solid curves). (**b**): EtBr+ DMAA alone (dashed curve) and after addition of APS or APS/TEMED (solid curves). (**c**): EtBr+ DMAA+DNA before (dashed curve) and after addition of APS or APS/TEMED (solid curves)

Scheme 2 Proposed scheme for the reaction of radicals with EtBr

TEMED, or both. EtBr alone exhibits an absorption maximum at 478 nm whereas a structureless spectrum appears upon addition of APS, which we attribute to the electrostatic interaction between anionic APS and cationic EtBr causing the alteration of conjugation on the structure [8]. Moreover, the addition of TEMED alone does not induce a spectral change but the addition of both APS and TEMED to the EtBr solution produces a large hypochromic shift to 430 nm in absorption maximum. Because TEMED is an accelerator for the decomposition of APS and able to generate free radical at or below the room temperature, this finding reveals that the radicals generated using APS + TEMED redox initiator system leads to an electron transfer, resulting in a reduction of EtBr (Scheme 2). Considering the fact that the formation of hydroethidine requires a two- electron transfer reaction that exhibits an absorption maximum at 350 nm [26], it was deduced that the observed product is novel and unfamiliar to our knowledge.

A similar hypochromic shift to 430 nm was also observed when APS or APS + TEMED were added to

10 μM EtBr solution containing DMAA monomer at a concentration of 1 M. The dashed curve in Fig. 1b presents the spectrum of aqueous EtBr + DMAA solution whereas the solid curves are the spectra after addition of APS and APS+ TEMED. Because APS and TEMED initiate the polymerization of DMA via free-radical mechanism, the appearance of the absorbance maximum at the same wavelength ($430 \pm$ 2 nm) reveals that the electron transfer mechanism from radical to EtBr was not affected due to the polymerization of DMAA. Interestingly, including ds-DNA in the aqueous solution of EtBr and DMAA, no hypechromic shift was observed, as seen in Fig. 1c. Instead, a bathochromic shift of about 50 nm in peak maximum of EtBr was observed when DNA was included to the EtBr- DMAA solution containing APS with or without TEMED. Noticeably, the peak maximum of EtBr at 530 nm unchanged in the presence of DNA, indicating that reduction of EtBr could not take place during the polymerization process due to intercalation between the strands of DNA. Hence, DNA-EtBr intercalation mechanism prevents the electron transfer to EtBr from free radicals in the system.

Fig. 2 Excitation spectra of 10 μM EtBr in different environments. (**a**) In water (**1**), upon addition of APS (**2**), APS + TEMED (**3**) and APS + TEMED + DNA (**4**). (**b**) In solution of 1 M DMAA (**1**), upon addition of APS (**2**), APS + TEMED (**3**) and APS + TEMED + DNA (**4**). $\lambda_{em} = 615$ nm
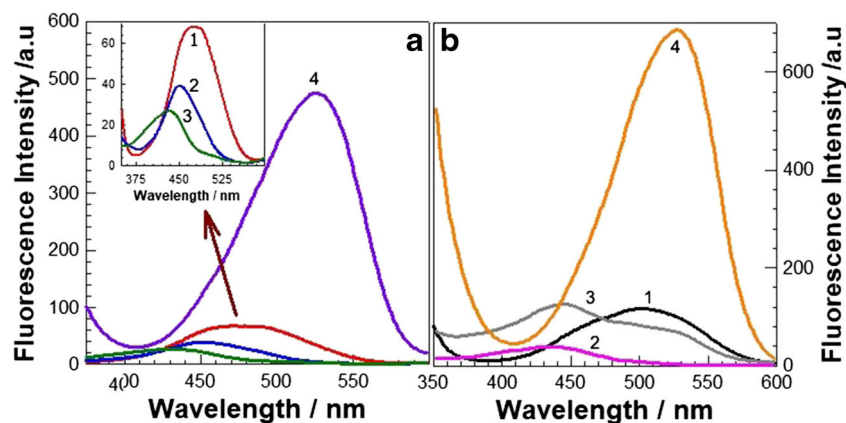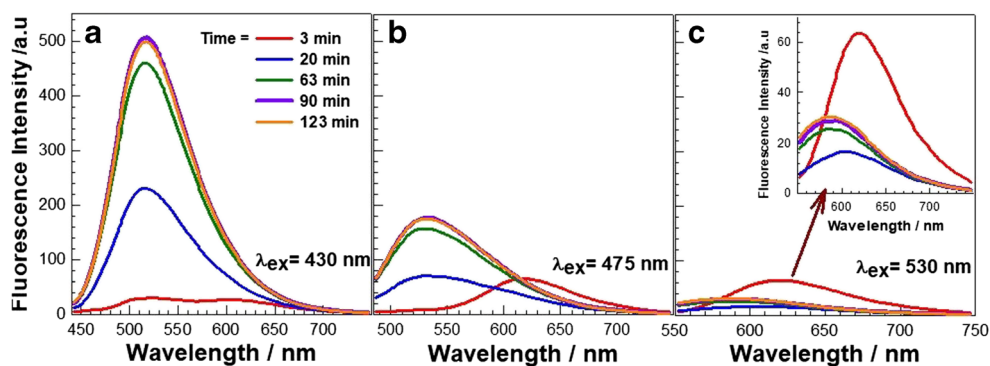
Fig. 3 Time-dependent emission spectra of FS formed during the reduction of 10 μM EtBr in pre-polymer solution containing DMAA+APS + TEMED depending on excitation wavelengths; (**a**) λ_{ex} = 430 nm, (**b**) λ_{ex} = 475 nm, (**c**) λ_{ex} = 530 nm. Time periods are indicated

Excitation Spectra of EtBr in the Presence of Different Species

Excitation spectrum of 10 μM aqueous EtBr solution is similar to absorption spectrum with displaying maximum at 475 nm (Fig. 2a). As seen from Fig. 2a, the wavelength of maximum intensity shifts to 450 nm upon addition of APS (curve 2) and there is no spectral change in the presence of only TEMED (data not shown) but shifts to 430 nm by addition of both APS and TEMED (curve 3). However, EtBr displays peak maximum at 500 nm in the presence of DMAA (Fig. 2b, curve 1), showing the hydrophobic environment formed around EtBr due to interaction with DMAA. After addition of APS into pre-polymer solution, there was a blue shift (70 nm) in maximum of wavelength (Fig. 2b, curve 2). Nevertheless, EtBr exhibits excitation maximum at both 440 nm with a shoulder at around 500 nm when both APS and TEMED were added (Fig. 2b, curve 3). The shoulder appears due to formation of a new product during the course of polymerization and vanishes after exhibiting a blue shift at the end of the reaction. Detailed explanation is given in the latter section and in the supporting information by presenting

the time dependent emission spectra. On the other side, the peak maximum of EtBr apparently red-shifted to 530 nm, following the addition of DNA to the pre-polymer solution with or without DMAA containing APS and TEMED (curve 4 in Fig. 2a and b). It is noticeable that the intercalation of EtBr between the strands of DNA is much stronger than the other interactions and intercalation was achieved for both systems with or without DMAA.

Fluorescence Spectra of EtBr during Reduction and Formation of FS

The emission spectra of EtBr during the reduction in 1 M DMAA solution containing APS and TEMED at various excitation wavelengths were monitored at different time periods prior to addition of all reagents (Fig. 3). Strikingly, at earlier times of polymerization, the peak maximum at 617 ± 2 nm diminishes and the peak appeared at 525 nm (λ_{ex} = 430 nm) starts to rise as the polymerization proceeds (Fig. 3a). The intensity of the peak at 525 nm depends on excitation wavelength and almost vanished when excited at 530 nm (Fig. 3a and b) showing that besides EtBr, another product also existed
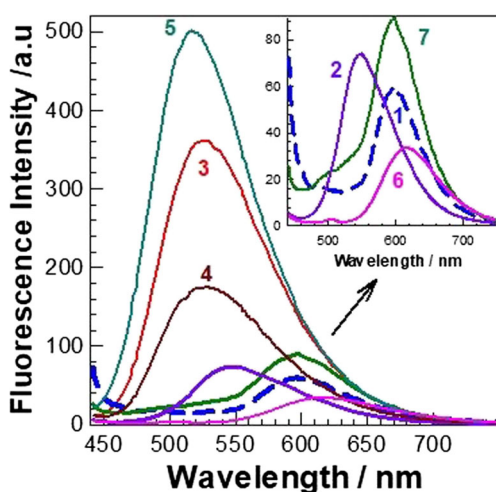

Fig. 4 Emission spectra of 10 μM aqueous EtBr solution (**1**), upon addition of APS (**2**), APS + TEMED (**3**), DMAA+APS (**4**), DMAA+APS + TEMED (**5**), DNA + APS + TEMED (**6**) DNA + DMAA+APS + TEMED (**7**). λ_{ex} = 430 nm)
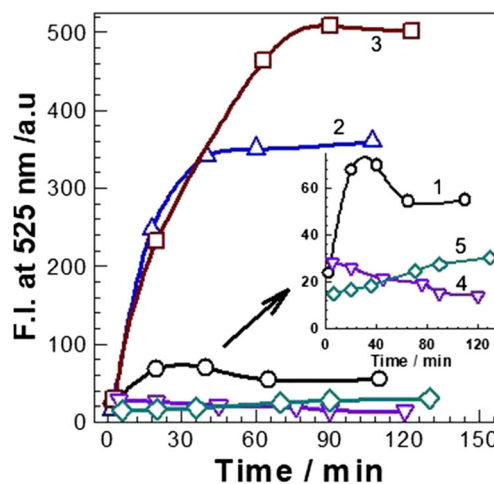

Fig. 5 Emission intensities at 525 nm as a function of time of 10 μM EtBr solution upon addition of APS (**1**), APS + TEMED (**2**), APS + TEMED+DMAA (**3**), APS + TEMED+DNA (**4**) and APS + TEMED+DMAA+DNA (**5**). λ_{ex} = 430 nm
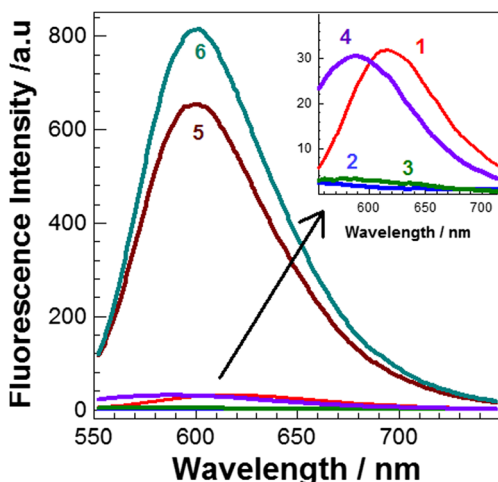
Fig. 6 Fluorescence spectra of 10 μM aqueous EtBr solution (**1**), upon addition of APS (**2**), APS + TEMED (**3**), APS + TEMED+DMAA(**4**), APS + TEMED+DNA(**5**) and APS + TEMED+DMAA+ DNA (**6**). $\lambda_{ex} = 530$ nm

Fig. 8 Variation of emission intensities at 500 nm of solutions (DMAA+ APS + TEMED) containing nanoclays; Laponite XLG (**1**) and Laponite XLS (**2**). ($\lambda_{ex} = 430$ nm). **Inset figure:** Intensities at 617 nm for same solutions upon excitation at 530 nm

in reaction solution. This result is indeed intriguing, considering that the fluorescence spectrum of EtBr in aqueous solution exhibits a maximum emission at 617 ± 2 nm which is independent from the time and the excitation wavelength as expected (Fig. S1).

In order to clarify that the new reduced product has distinct characteristics from HE, both EtBr and HE in DMSO solutions were excited at 350 nm and they exhibited emission maxima at 640 and 420 nm respectively (Fig. S2). Figure 4 shows the fluorescence spectra of EtBr itself and after the reagents added individually into the aqueous solution was obtained by excitation at 430 nm after a waiting time up to 120 min to ensure that all interactions or reactions between the species were ended (from Fig. S3 to Fig. S8).

Nevertheless, there seems to be change in spectrum of EtBr after addition of APS and the peak maximum shifts to 542 ± 2 nm (Fig. 4 curve 2 and Fig. S3). A new peak with a maximum of 525 nm appeared after addition of both APS and TEMED (Fig. 4, curve 3). Moreover, the emission intensity of peak at 525 nm, which might be ascribed to FS, gradually increased depending on time (Fig. S4).

Meanwhile, the spectrum obtained upon exciting at 475 nm exhibits the emissions at 600 and 530 nm, indicating that both EtBr and the formed product exist in solution (Fig.S4). Fluorescence spectra of EtBr upon excitation at 430 nm exhibit maximum peak at 518 nm during the polymerization of DMAA initiated by APS with or without TEMED (Fig. 4, curve 4 and 5), whereas there was no emission peak around 530 nm (Fig. 4, curves 6 and 7) in the presence of DNA with or without DMAA upon excitation wavelengths (Fig.S7 and Fig. S8). This indicates that either the interaction of DNA with EtBr creates the hydrophobic environment or EtBr intercalates into DNA and therefore prevents the process of reduction.

Figure 5 shows the emission intensities at 525 ± 2 nm of all samples as a function of time. In the presence of only APS, there seems to be a small increment in emission intensity, whereas there is an apparent rise of intensity in the presence of APS and TEMED, showing the formation of a reduced product.

Addition of DMAA into this mixture results in a further increase in emission intensity (Fig. 5, curve with squares). This may be due to the two reasons: first, the concentration of reduced product increases upon polymerization of DMAA

Fig. 7 Time dependent fluorescence spectra of the formation of fluorescent species during reduction of EtBr in aqueous solution containing DMAA, APS, TEMED and Laponite XLG upon three different excitation wavelengths. Time scales and excitation wavelengths are indicated
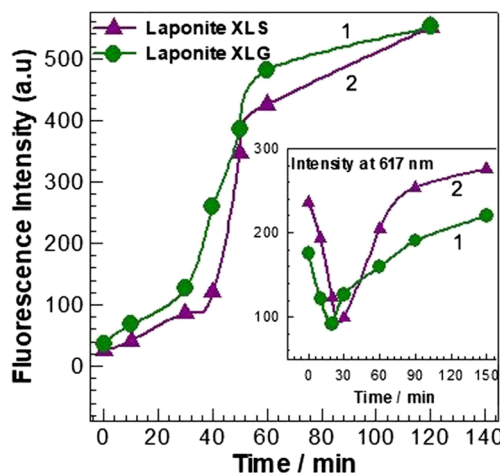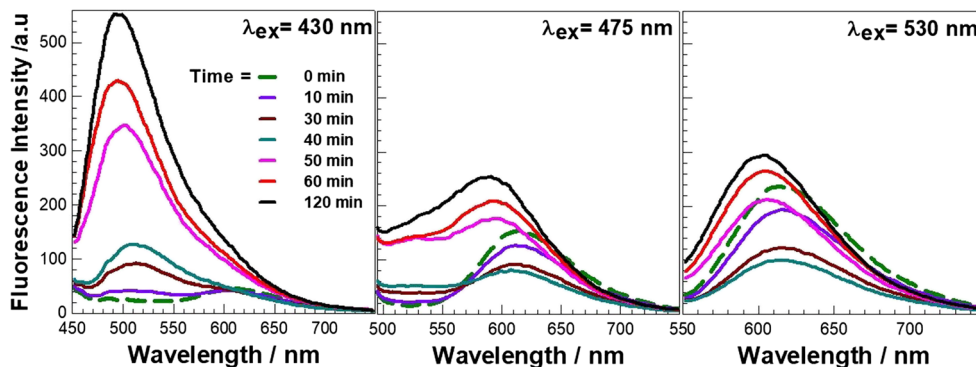
Samples	Absorption maxima (nm)	Emission maxima (nm)	Quantum yield
EtBr	480	617	0.022
EtBr+APS + TEMED	430	525	0.148
EtBr+DMAA+APS	430	525	0.106
EtBr+DMAA+APS + TEMED	430	525	0.207

Table 1 Photophysical properties of EtBr in different environments[a]

a: EtBr = 10 μM, DMAA = 1 M, APS = 3.51 mM, TEMED = 0.08 v/v%, Laponite XLG = 3 w/v %

and second, formation of poly(DMAA) creates a more rigid environment by means of increasing the dynamic viscosity of the reaction system, resulting in enhancement of fluorescence emission intensity. Note that no emission peak observed around 530 nm when excited at 430 nm (Fig. 5, curves with triangles down and diamonds respectively) in the presence of DNA whether DMAA is included or not (Fig.S7 and Fig. S8). This is evidence that the intercalation of EtBr with DNA does not allow APS to reach EtBr for electron donation.

In the presence of a reducing agent, the change in the fluorescence emission of EtBr can provide information to evaluate the structure of DNA-intercalator complex. Therefore, we used different excitation wavelengths in order to figure out the environment of EtBr upon interaction with DNA (Fig. 6). As seen, existence of emission at 600 nm upon excitation at 530 nm indicates that polymerization of DMAA creates hydrophobic environment around EtBr and retards the reduction of EtBr to some extent. On the other hand, binding of EtBr by intercalating between DNA base pairs may also inhibits the reduction process (Fig. 6).

Nanoclay Effect on FS during Reduction of EtBr

The fluorescence spectra of EtBr in pre-gel solution containing DMAA, APS, TEMED and nanoclays XLG (Fig. 7) and
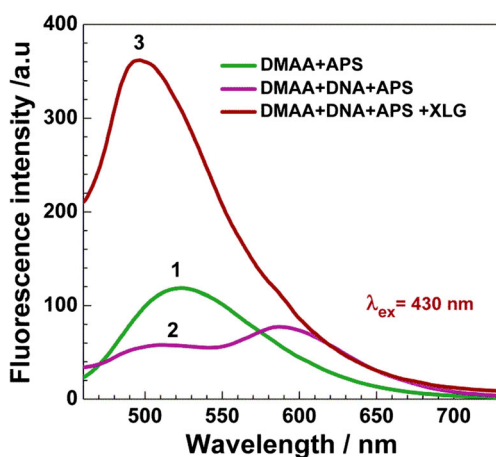
Fig. 9 Fluorescence spectra of 10 μM EtBr at 55 °C in the presence of APS after polymerization of DMAA (**1**), with DNA added (**2**), with both of DNA and Laponite XLG added (**3**)

XLS (Fig.S9) were recorded depending on time upon three different excitation wavelengths. The existence of different emission maxima in fluorescence spectra indicates that dissimilar species exist in solution in the presence of the radical producing agent APS or upon polymerization of DMAA. When excited at 430 nm, maximum in fluorescence spectrum (617 ± 2 nm) belonging to EtBr in hydrophilic environment, blue-shifted to 500 nm, showing that reduction of EtBr results in creation of a fluorescent product. The emission intensity of EtBr in the presence of both XLG and XLS at 500 nm enhanced by increasing the polymerization time (Fig. 8). However, emission intensity of EtBr at 617 nm decreases first and then increased depending on time. This might be due to the charge neutralization of EtBr upon electrostatic interaction with clays first and then starting of gel formation in the system. When emission intensities were plotted against the polymerization time, turning point in curve is 40 min for XLG and 20 min for XLS (Fig. 8, inset).

The Fluorescence Quantum Yield of Treated Samples of EtBr

The quinine sulfate was used as a standard (Φ_{ref} = 0.54 in 0.1 N H_2SO_4) in order to determine the fluorescence quantum yield of EtBr in each sample. Fluorescence quantum yield was calculated according to the following equation [26].

$$\Phi_s = \Phi_{ref}\left(\frac{F_s}{F_{ref}}\right)\left(\frac{A_{ref}}{A_s}\right)\left(\frac{n_s^2}{n_{ref}^2}\right) \tag{1}$$

where F_s and F_{ref} are integrated area under the fluorescence emission spectrum measured of sample and standard, respectively; A_s and A_{ref} are absorbances at the same excitation wavelength of sample and standard, respectively; n_s and n_{ref} are refractive indexes of solvent used for sample and standard, and Φ_{ref} is quantum yield of standard. Fluorescence quantum yields of each sample were shown in Table 1.

Maximum wavelength of EtBr at 617 ± 2 nm in aqueous solution at 25 °C shifted to 520 nm after completion of DMAA polymerization by using only APS as an initiator at 55 °C (Fig. 9). This means that fluorescent product is also formed by reduction of EtBr in the absence of TEMED. On

the other hand, when polymerization reaction was carried out in the presence of DNA, fluorescence spectrum with double emission maxima at both around 510 nm and 600 nm was obtained. The emission peak at 600 nm shows the existence of unreduced EtBr, whereas there was no any peak formation at 510 nm in the presence of DNA when the polymerization was carried out in the presence of both APS and TEMED at 25 °C. Meanwhile, addition of XLG to pre-polymer solution in the presence of DNA caused to increase in peak intensity at around 500 nm. These results revealed that polymerization temperature and existence of XLG might tear off EtBr intercalated with DNA and lead to reduction of EtBr.

Conclusions

We have found that EtBr was converted into a new fluorescent signal (FS) during the radical polymerization of DMAA. The photophysical property of product formed is completely different from HE, which is two-electron reduced product of EtBr. The results revealed that EtBr partially reduced and FS formed in gel containing nanoclays since each different excitation resulted in specific fluorescence spectra. However, there was no formation of reduced product in the presence of DNA, indicating that intercalative binding of DNA creates shielding effect on EtBr to protect from reduction. Although DNA protects EtBr from being reduced, the transfer of electron to EtBr occurred by addition of nanoclay (Laponite XLG or XLS) into the pre-polymer solution when polymerization was carried out at 55 °C. The fluorescence measurements after polymerization of DMAA in the presence of DNA and nanoclay at 55 °C revealed that the conformation of DNA was changed, allowing the electrostatic interaction of EtBr with nanoclay. This indicates the weakening of intercalative binding which originates from partial destruction of double helix structure of DNA upon heating. These findings might lead the way to future research about elucidation of conformational change of DNA depending on change in temperature or upon interaction with molecules. Besides, the nanoclay interacted with EtBr by electrostatically could not protect EtBr from being reduced. This indicates that electrostatic interaction with DNA through phosphate backbone could not contribute the protection of EtBr from electron transfer process, whereas intercalative binding of EtBr to DNA creates barrier to shield EtBr from reduction process. The experimental data generated through the spectrophotometric techniques employed herein are of great importance since they allow a better understanding of instant formation of FS and can aid future studies on new systems specially designed for investigation on structural change in conformation of DNA.

References

1. Lavis LD, Raines RT (2008) Bright ideas for chemical biology. ACS Chem Biol 3:142–155
2. Terai T, Nagano T (2008) Fluorescent probes for bioimaging applications. Curr Opin Chem Biol 12:515–521
3. Wysocki LM, Lavis LD (2011) Advances in the chemistry of small molecule fluorescent probes. Curr Opin Chem Biol 15:752–759
4. Chib R, Raut S, Sabnis S, Singhal P, Gryczynski Z, Gryczynski I (2014) Associated anisotropy decays of ethidium bromide interacting with DNA. Methods Appl Fluoresc 2
5. Mukherjee A, Singh B (2017) Binding interaction of phatinaceutical drug captopril with calf thymus DNA: a multispectroscopic and molecular docking study. J Lumin 190:319–327
6. Liu BM, Bai CL, Zhang J, Liu Y, Dong BY, Zhang YT, Liu B (2015) In vitro study on the interaction of 4,4-dimethylcurcumin with calf thymus DNA. J Lumin 166:48–53
7. Roy S, Saxena SK, Mishra S, Yogi P, Sagdeo PR, Kumar R (2018) Spectroscopic evidence of phosphorous heterocycle-DNA interaction and its verification by docking approach. J Fluoresc 28:373–380
8. Cosa G, Focsaneanu KS, McLean JRN, McNamee JP, Scaiano JC (2001) Photophysical properties of fluorescent DNA-dyes bound to single- and double-stranded DNA in aqueous buffered solution. Photochem Photobiol 73:585–599
9. Sun YT, Peng TT, Zhao L, Jiang DY, Cui YC (2014) Studies of interaction between two alkaloids and double helix DNA. J Lumin 156:108–115
10. Paramanik B, Bhattacharyya S, Patra A (2013) Steady state and time resolved spectroscopic study of QD-DNA interaction. J Lumin 134:401–407
11. Yuvaraj M, Aruna P, Koteeswaran D, Tamilkumar P, Ganesan S (2015) Rapid fluorescence spectroscopic characterization of salivary DNA of normal subjects and OSCC patients using ethidium bromide. J Fluoresc 25:79–85
12. Geng SQ, Wu Q, Shi L, Cui FL (2013) Spectroscopic study one thiosemicarbazone derivative with ctDNA using ethidium bromide as a fluorescence probe. Int J Biol Macromol 60:288–294
13. Zhou XY, Zhang GW, Wang LH (2014) Binding of 8-methoxypsoralen to DNA in vitro: monitoring by spectroscopic and chemometrics approaches. J Lumin 154:116–123
14. Agarwal S, Jangir DK, Mehrotra R (2013) Spectroscopic studies of the effects of anticancer drug mitoxantrone interaction with calf-thymus DNA. J Photochem Photobiol B Biol 120:177–182
15. Rafique B, Khalid AM, Akhtar K, Jabbar A (2013) Interaction of anticancer drug methotrexate with DNA analyzed by electrochemical and spectroscopic methods. Biosens Bioelectron 44:21–26
16. Temerk Y, Ibrahim M, Ibrahim H, Kotb M (2015) Interactions of an anticancer drug Formestane with single and double stranded DNA at physiological conditions. J Photochem Photobiol B Biol 149:27–36
17. Xia KX, Zhang GW, Li S, Gong DM (2017) Groove binding of vanillin and ethyl vanillin to calf Thymus DNA. J Fluoresc 27:1815–1828
18. Benov L, Sztejnberg L, Fridovich I (1998) Critical evaluation of the use of hydroethidine as a measure of superoxide anion radical. Free Radic Biol Med 25:826–831
19. Budd SL, Castilho RF, Nicholls DG (1997) Mitochondrial membrane potential and hydroethidine-monitored superoxide generation in cultured cerebellar granule cells. FEBS Lett 415:21–24
20. Zhao H, Kalivendi S, Zhang H, Joseph J, Nithipatikom K, Vásquez-Vivar J, Kalyanaraman B (2003) Superoxide reacts with

hydroethidine but forms a fluorescent product that is distinctly different from ethidium: potential implications in intracellular fluorescence detection of superoxide. Free Radic Biol Med 34:1359–1368

21. Zielonka J, Kalyanaraman B (2010) Hydroethidine- and MitoSOX-derived red fluorescence is not a reliable indicator of intracellular superoxide formation: another inconvenient truth. Free Radic Biol Med 48:983–1001

22. Kalyanaraman B, Dranka BP, Hardy M, Michalski R, Zielonka J (2014) HPLC-based monitoring of products formed from hydroethidine-based fluorogenic probes - the ultimate approach for intra- and extracellular superoxide detection. Biochim Biophys Acta-General Subjects 1840:739–744

23. Maghzal GJ, Cergol KM, Shengule SR, Suarna C, Newington D, Kettle AJ, Payne RJ, Stocker R (2014) Assessment of myeloperoxidase activity by the conversion of hydroethidine to 2-chloroethidium. J Biol Chem 289: 5580–5595

24. Michalski R, Michalowski B, Sikora A, Zielonka J, Kalyanaraman B (2014) On the use of fluorescence lifetime imaging and dihydroethidium to detect superoxide in intact animals and ex vivo tissues: a reassessment. Free Radic Biol Med 67:278–284

25. Thomas G, Roques B (1972) Proton magnetic-resonance studies of ethidium bromide and its sodium-borohydride reduced derivative. Febs Lett 26:169–175

26. Phukan S, Mitra S (2012) Fluorescence behavior of ethidium bromide in homogeneous solvents and in presence of bile acid hosts. J Photochem Photobiol A Chem 244:9–17